THE JOURNAL OF BIOLOGICAL CHEMISTRY VOL. 281, NO. 36, pp. 26444–26454, September 8, 2006

State-dependent Conformations of the Translocation Pathway in the Tyrosine Transporter Tyt1, a Novel Neurotransmitter:Sodium Symporter from *Fusobacterium nucleatum*[*]

Received for publication, March 15, 2006, and in revised form, May 18, 2006 Published, JBC Papers in Press, June 23, 2006, DOI 10.1074/jbc.M602438200

Matthias Quick[‡], Hideaki Yano[‡], Naomi R. Goldberg[‡], Lihua Duan[‡], Thijs Beuming[§], Lei Shi[§], Harel Weinstein[§¶], and Jonathan A. Javitch[‡‖1]

From the [‡]Center for Molecular Recognition and [‖]Departments of Psychiatry and Pharmacology, Columbia University College of Physicians and Surgeons, New York, New York 10032 and [§]Department of Physiology and Biophysics and [¶]His Royal Highness Prince Alwaleed Bin Talal Bin Abdulaziz Alsaud Institute for Computational Biomedicine, Weill Medical College of Cornell University, New York, New York 10021

The gene of a novel prokaryotic member (Tyt1) of the neurotransmitter:sodium symporter (NSS) family has been cloned from *Fusobacterium nucleatum.* In contrast to eukaryotic and some prokaryotic NSSs, which contain 12 transmembrane domains (TMs), Tyt1 contains only 11 TMs, a characteristic shared by ~70% of prokaryotic NSS homologues. Nonetheless upon heterologous expression in an engineered *Escherichia coli* host, Tyt1 catalyzes robust Na^+-dependent, highly selective L-tyrosine transport. Genetic engineering of Tyt1 variants devoid of cysteines or with individually retained endogenous cysteines at positions 18 or 238, at the cytoplasmic ends of TM1 and TM6, respectively, preserved normal transport activity. Whereas cysteine-less Tyt1 was resistant to the inhibitory effect of sulfhydryl-alkylating reagents, *N*-ethylmaleimide inhibited transport by Tyt1 variants containing either one or both of the endogenous cysteines, and this inhibition was altered by the substrates sodium and tyrosine, consistent with substrate-induced dynamics in the transport pathway. Our findings support a binding model of Tyt1 function in which an ordered sequence of substrate-induced structural changes reflects distinct conformational states of the transporter. This work identifies Tyt1 as the first functional bacterial NSS member putatively consisting of only 11 TMs and shows that Tyt1 is a suitable model for the study of NSS dynamics with relevance to structure/function relationships of human NSSs, including the dopamine, norepinephrine, serotonin, and γ-aminobutyric acid transporters.

Na^+/Cl^--dependent neurotransmitter transporters fulfill an essential role in the nervous system by terminating synaptic transmission and recycling neurotransmitters for reuse (1, 2). These proteins are secondary active transporters that utilize the Na^+ electrochemical gradient across the plasma membrane of the presynaptic neuron or glia to catalyze the (re)uptake of a variety of neurotransmitters from the extracellular milieu against their concentration gradient in a cotransport (symport) mechanism (3–5). Hence they are referred to as neurotransmitter:sodium symporters (NSSs)[2] (6). Substrates of NSSs include biogenic amines, such as dopamine, norepinephrine, and serotonin, as well as amino acids (γ-aminobutyric acid, glycine, and proline) and osmolytes (betaine and creatine) (Ref. 7; for recent reviews, see Refs. 8 and 9). The transporters for the biogenic amines dopamine, norepinephrine, and serotonin (DAT, NET, and SERT, respectively) are of particular interest because they are targets for the action of numerous drugs, including the widely abused psychostimulants cocaine and amphetamine (10), as well as for antidepressant drugs (11).

Although some mechanistic features of a variety of cloned members of the NSS family (GAT (12), DAT (13), SERT (14), and NET (15)) have been elucidated in eukaryotic expression systems, these systems are not well suited for large scale expression and purification of these transporters (16, 17). To obtain information on the structure and function of membrane proteins, prokaryotic homologues can be extremely valuable because recombinant transporters can be expressed in bacteria in large quantities (18), a prerequisite for their subsequent purification and biochemical/biophysical analyses (19, 20).

Recently the structure of a bacterial NSS homologue, LeuT of *Aquifex aeolicus*, was solved using such an approach (21). The availability of this structure is a major advance with wide ramifications for the field. The structure of LeuT is of a substrate-bound "closed" state blocking access of substrate to either side of the membrane. The structure provides only limited clues to the location of the transport pathway, and additional structural and functional information will be vital to determining the location of the transport pathway and the conformational changes involved in the transport cycle. Ironically LeuT was crystallized

[*] This work was supported by National Institutes of Health Grants MH57324 and DA17293 (to J. A. J.) and DA12408 (to H. W. and J. A. J.). The costs of publication of this article were defrayed in part by the payment of page charges. This article must therefore be hereby marked "*advertisement*" in accordance with 18 U.S.C. Section 1734 solely to indicate this fact.

[1] To whom correspondence should be addressed: Center for Molecular Recognition, Columbia University College of Physicians and Surgeons, P&S 11-401, Box 7, New York, NY 10032. Tel.: 212-305-7308; Fax: 212-305-5594; E-mail: jaj2@columbia.edu.

[2] The abbreviations used are: NSS, neurotransmitter:sodium symporter; DAT, dopamine transporter; GAT, γ-aminobutyric acid transporter; Mes, 2-(*N*-morpholino)ethanesulfonic acid; NEM, *N*-ethylmaleimide; NET, norepinephrine transporter; SERT, serotonin transporter; TM, transmembrane domain; CL, Cys-less; WT, wild type; SGLT, sodium/glucose transporter; MelB, melibiose permease of *Escherichia coli*.

successfully in part because it is so tightly bound to substrate. Although this is a clear advantage for crystallization, it is a disadvantage for reconstitution and functional studies, which require addition and removal of substrates. Indeed the published value for transport velocity per milligram of protein with reconstituted LeuT (21) is several orders of magnitude slower than that seen in other NSSs (*e.g.* $\sim$0.5 s^{-1} for human DAT (22) and $\sim$5 s^{-1} for rat GAT (23)), suggesting the need for other bacterial NSS proteins that may be more amenable to studies of transporter dynamics.

Here we report the functional characterization of a novel prokaryotic member of the NSS family, the Na^+-dependent tyrosine transporter (Tyt1) of *Fusobacterium nucleatum* heterologously expressed in *Escherichia coli*. This transporter is the first characterized NSS homologue predicted to have only 11 transmembrane segments and is therefore representative of more than 180 novel prokaryotic NSS members that can now be predicted also to function as sodium-dependent transporters. We also present biochemical studies which, interpreted in the structural context of a LeuT-based molecular model, serve to elucidate substrate-induced alterations in the transporter structure and identify elements of the transport pathway.

EXPERIMENTAL PROCEDURES

Cloning of the tyt1 Gene—The gene of the proposed sodium-dependent tyrosine transporter (designated *tyt1* hereafter) of *F. nucleatum* (GenBank™ accession number NP_602780) was PCR-amplified from genomic DNA generously provided by Dr. Susan Kinder Haake (UCLA School of Dentistry) using the following primers: tyt1_s, GTACAAAAAAGCAGGCT*CCATGG*ACAATTCGGAAAGGAAGTTTCAGTC (the NcoI restriction site is shown in italic); and tyt1_as, GCTCAGCTAATTAAGCTGTACAAGAAAGCTGGGT*AAGCTT*ATCCAATACC (the HindIII restriction site is shown in italic). The resulting PCR product contained the entire *tyt1* gene flanked by unique NcoI and HindIII restriction sites at the 5′- and 3′-ends, respectively. Using these sites, the amplified fragment was introduced into a derivative of pT7-5 (24), and the fidelity of the insert was confirmed by DNA sequencing (ABI 310 automated sequencer; Columbia University DNA facility). For overproduction of Tyt1 via the inducible T5 promoter, *tyt1* was cut with NcoI/HindIII and subcloned into a similarly digested derivative of pQE60 (Qiagen) containing a 10-histidine coding region before the *tyt1* start codon (N-terminal amino acid sequence of recombinant Tyt1: $MS[H]_{10}[D]_4KA\underline{MDNS}$; native amino acid residues 1–4 of Tyt1 are underlined). The resulting plasmid was designated pQ2.

Bacterial Strains—*E. coli* XL1Blue (*recA1 endA1 gyrA96 thi-1 hsdR17 supE44 relA1 lac* (F′*proAB lacI*^{q}*ZΔM15 Tn10* (Tet^r))) (Stratagene) served as host strain for basic cloning purposes and plasmid isolation. *E. coli* CY15212 (SVS1144 *mtr aroP tnaB271*::Tn5) (25) was used as parental strain for the engineering of a suitable *E. coli* host, MQ614 (CY15212 *tyrP1 pheP*::*cat*) that is devoid of all known intrinsic aromatic amino acid uptake systems (see below). *E. coli* MQ614 harboring the indicated plasmids was used for the *in vitro* characterization of tyrosine transport kinetics and biochemical studies.

Generation of E. coli MQ614—Chromosomal gene disruption in *E. coli* CY15212 (*mtr*$^-$ *aroP*$^-$ *tnaB*$^-$) was performed according to the method of Datsenko and Wanner (26) using the "gene disruption kit" obtained from the Yale *E. coli* Stock Center. For each disruption cycle cells of CY15212 (and derivatives) were transformed with pKD46 as the Red-recombinase expression plasmid by electroporation. After antibiotic screening of successful clones, the antibiotic resistance gene was eliminated by transforming the cells with the FLP helper plasmid pCP20. Chromosomal deletions of the *tyrP* and *pheP* genes were sequentially introduced using the following primers: tyrP_s, GCAGATATCACTCATAAAGATCGTCAGGACAGAAGAAAGCGTGAAAAACAGAACCC*GTGTAGGCTGGAGCTGCTTC*; tyrP_as, CCCCACTTCTGGTAACAACCCTGCCGCAATCAAAAATTGCACGCC*CATATGAATATCCTCCTTA*; pheP_s, CCTCAACAAAAAAGACACACAGGGGAAAGGCGTGAAAAACGCGTCAACCGTATCGGAAG*GTGTAGGCTGGAGCTGCTTC*; pheP_as, GCAGAGATAGTTGCCGAACGGATAGAGCAGCGCCTTAAACTGTGTTTCACGCCCCC*CATATGAATATCCTCCTTA* (P1 and P2 sites are shown in italic), and pKD3 as template plasmid. After isolating the genomic DNA from the respective *E. coli* knock-out strain (DNeasy kit, Qiagen) the elimination of the target gene was confirmed by agarose gel electrophoresis of PCR-amplified DNA fragments that enclosed the target region. Genomic DNA of the parental strain CY15212 served as a control.

Site-directed Mutagenesis—Site-directed replacement of the two intrinsic cysteine residues in Tyt1 (Cys-18 and Cys-238) was performed using a two-step PCR protocol (27) with pQ2 as template. For each pair of mutagenic primers the sense primer is presented with the altered nucleotides underlined: C18A, GGTTTCATTTTAACT$\underline{GC}$TGTTGGATCTGC; C238F, GGAATGATAGTCT$\underline{TC}$GGAGCATACTTAG. The resulting PCR fragments were digested with NcoI/HindIII and inserted individually into similarly cut pQ2 to generate pQ2-C18A or pQ2-C238F (encoding Tyt1 with a single cysteine at amino acid position 238 or 18, respectively). After verification of the DNA integrity by sequencing of the resulting plasmids, a cysteine-free version of Tyt1 (Tyt1-CL) was engineered by combining the corresponding fragments of pQ2-C18A and pQ2-C238F using a suitable restriction enzyme combination. Substitution of Gly-24 with Asp was performed in a single step PCR using mutagenic oligo G24D, CAGT*CCATGG*ACAATTCGGAAAGGAAGTTTCAGTCAAAAATAGGTTTCATTTTAACTTGTGTTGGATCTGCTGTTG$\underline{AC}$ATGG (altered nucleotides are underlined; the NcoI restriction site is shown in italic), with pQ2 as template. The modified *tyt1* gene was introduced by means of an NcoI/HindIII digest into pQ2, and its correctness was verified by sequencing.

Transport Assay—Active transport was measured in *E. coli* MQ614 (*aroP mtr tnaB tyrP1 pheP*::*cat*) transformed with derivatives of pQ2 encoding Tyt1 with the indicated amino acid replacements. The cells were grown aerobically in Luria-Bertani medium (28) containing 100 μg/ml ampicillin at 37 °C. Overnight cultures were diluted 50-fold and were allowed to grow to an optical density at 420 nm of 1.0 followed by induction of gene expression by addition of 0.15 mM isopropyl 1-thio-β-D-galactopyranoside for 2 h. Cells were harvested by centrif-

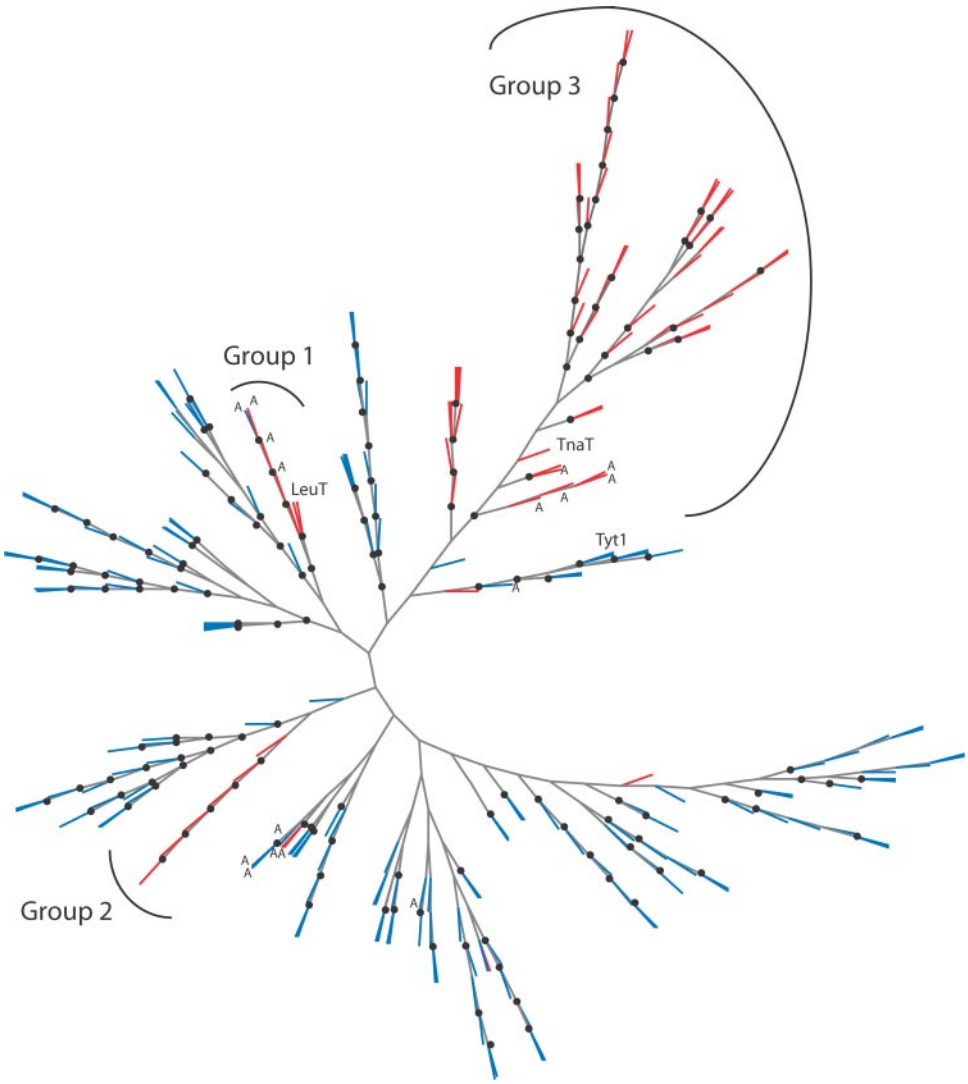

FIGURE 1. **Phylogenetic tree of 252 prokaryotic NSS proteins.** The PHYLIP package (Version 3.65 (62)) was used. The trees were calculated with the maximum parsimony method implemented in *protpars*. The final consensus tree was determined by "majority rule (extended)" consensus method in *consense* and is based on a bootstrapped parsimony analysis (1,000 replicas, data sets were generated with *seqboot*). The branches with bootstrap values higher than 50% are indicated with *black dots* at the *forks*. To improve bootstrap values, only the TM regions were included because they could be unambiguously aligned. To facilitate comparison with 11-TM NSS proteins, only the first 11 TMs of the 12-TM family members were considered. *Leaves* representing NSS proteins with 12 TMs are shown in *red*, whereas *blue leaves* represent NSS proteins with only 11 TMs. Archaeal sequences are indicated with the letter *A*. LeuT, TnaT, and Tyt1 are indicated. Note that rather than being distributed throughout the entire tree, most of the prokaryotic 12-TM transporters are clustered in three groups, a large one of 52 and two small ones of seven, suggesting that the number of TMs is a conserved property of distinct subfamilies of prokaryotic NSS proteins.

ugation at 12,000 × *g* for 10 min and washed four times with 50 mM Tris/Mes, pH 7.5, at 4 °C to eliminate Na^+ contamination (29). For routine uptake experiments, cells were diluted in 50 mM Tris/Mes, pH 8.5 to a total protein concentration of 0.125 mg/ml. Transport of 0.1 μM L-[ring-3,5-^{3}H]tyrosine (54 Ci/mmol), L-[1-^{14}C]tyrosine (434 Ci/mol) (Moravek Biochemicals), or [ring-3,5-^{3}H]tyramine (50 Ci/mmol) (American Radiolabeled Chemicals, Inc.) was assayed in the presence of 10 mM NaCl (unless otherwise noted) at 23 °C for the indicated time periods using a rapid filtration method (30). Kinetics of sodium-dependent tyrosine transport of Tyt1 wild type and variants were determined by measuring the initial portion of the time course at different L-tyrosine concentrations (*i.e.* 10 s). The maximal velocity (V_{max}^{Tyr}) and apparent affinity constant at half-maximum velocity ($K_{0.5}^{Tyr}$) of tyrosine transport was determined by varying the L-[1-^{14}C]tyrosine concentration from 0.01 to 5 μM in the presence of 10 mM NaCl. For the determination of the apparent Na^+ activation constant ($K_{0.5}^{Na^+}$) of tyrosine transport (0.1 or 1 μM final L-[1-^{14}C]tyrosine concentration), the NaCl concentration was increased from virtually Na^+-free to 10 mM and was replaced with equimolar Tris/Mes to maintain a constant molarity of 60 mM.

Inhibition of Tyrosine Transport by Thiol Reagents—E. coli MQ614 harboring pQ2 or derivatives encoding Tyt1 wild type (WT), Tyt1-CL, Tyt1-C18A, or Tyt1-C238F was cultivated and treated as described above (see "Transport Assay"). Prior to transport, cells were incubated in the presence of *N*-ethylmaleimide (NEM) for 5 min in the presence or absence of substrate at 23 °C. The NEM concentration for each cysteine-containing Tyt1 variant was chosen to inhibit tyrosine transport by ~95% in the absence of substrate. Unbound NEM was removed by washing the cells three times with the incubation buffer (without NEM) followed by a wash with 50 mM Tris/Mes, pH 7.5. For transport studies treated cells were diluted in 50 mM Tris/Mes, pH 8.5, and uptake of 0.1 μM L-[1-^{14}C]tyrosine was measured for 1-min time intervals in the presence of 10 mM NaCl as described above.

Data Analysis—All experiments were repeated at least three times with cells from different cultures. Figures are based on data obtained from a typical experiment, and, unless otherwise noted, data points represent the mean of a triplicate determination ±S.D. (note that error bars are not always detectable due to the size of the symbols). Data fits of kinetic analyses were performed using the non-linear regression algorithm in Prism (Version 4.03, GraphPad Software, Inc.), and errors represent the S.E. of the fit.

RESULTS

The sequences of 252 prokaryotic NSS proteins were obtained from the National Center for Biotechnology Information RefSeq data base through a PSI-BLAST (position-specific

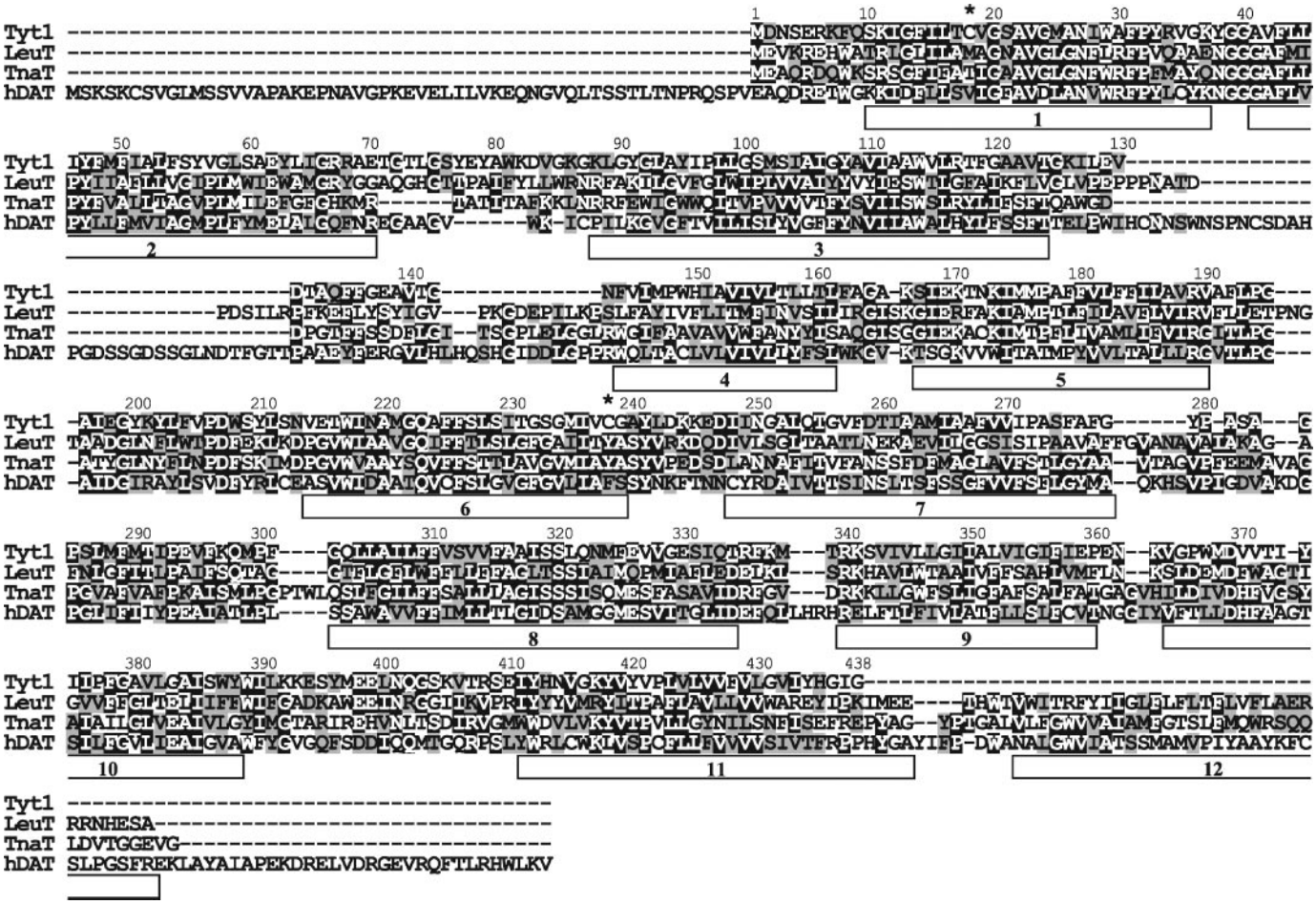

FIGURE 2. **Sequence alignment.** The sequences of human DAT (*hDAT*), TnaT of *Symbiobacterium thermophilum*, LeuT of *A. aeolicus*, and Tyt1 of *F. nucleatum* were aligned by ProbCons (63) followed by manual adjustment. Identical residues are highlighted with *black background*, while conserved amino acid substitutions (sequence similarity) are indicated by *gray background*. Transmembrane segments are indicated as *rectangles* based on the LeuT structure (21) and numbered using *Arabic numerals*. *Asterisks* indicate endogenous cysteine residues 18 and 238 (index positions 1.39 and 6.65, respectively (38)) in Tyt1.

iterated basic local alignment search tool) search. Initial predictions of the number and location of the TM segments in these 252 prokaryotic NSS proteins were obtained from topology predictions with the algorithms HMMTOP (31) and TMHMM (32). These predictions were corrected by visual inspection of the predicted TM boundaries based on a complete alignment of prokaryotic and eukaryotic NSS members.[3] Of the 252 prokaryotic NSS proteins that were considered, ~28% (71 including TnaT and LeuT) were predicted to have TMs 1–12, whereas ~72% (181 including Tyt1; see below) were predicted to have TMs 1–11 but lack a 12th TM. This is in marked contrast with eukaryotic NSS proteins where virtually all members have 12 TMs (data not shown). It was not previously known whether NSS proteins can function without TM12 and thus whether this large set of prokaryotic NSS sequences encode pseudogenes or functional proteins.

To determine whether prokaryotic NSS proteins with either 11 or 12 TMs belong to different subfamilies, the prediction results were plotted on a phylogenetic tree (Fig. 1) calculated with a maximum parsimony method (PHYLIP package, see legend to Fig. 1). Most of the 71 prokaryotic 12-TM transporters are clustered in three groups, two of seven (groups 1 and 2) and one of 52 (group 3), rather than distributed throughout the entire tree. In addition, although the 11-TM NSS proteins are relatively diverse, the node support for the 12-TM members is strong (bootstrap value of 89% for the major 12-TM cluster). Thus, the number of TMs is a conserved property of distinct subfamilies of prokaryotic NSS proteins as there are very few examples of homologues that are very similar in sequence but different in the number of TMs. Notably the majority of archaeal sequences (12 of 17) have 12 TMs.

To compare the sequence similarity between the 12-TM and 11-TM subfamilies, pairwise sequence identities were calculated from the alignment of these 252 prokaryotic NSS proteins. For the 11-TM and 12-TM subfamilies, the average similarity within the group is similar (33% in 11-TM and 35% in 12-TM subfamilies). The 11-TM and 12-TM subfamilies exhibit the same level of intragroup similarity (33% in 11-TM and 35% in 12-TM subfamilies). However, the average similarity is significantly lower (24%) between the two subfamilies, suggesting again that NSS proteins with 11 and 12 TMs represent distinct subfamilies.

Two bacterial members of the 12-TM family, TnaT (33) and LeuT (21), have been shown to be sodium-dependent

[3] T. Beuming, L. Shi, J. A. Javitch, and H. Weinstein, submitted.

tryptophan and leucine transporters, respectively. However, it was not known whether the ~70% of prokaryotic NSS proteins with 11 TM segments are functional transporters. Fig. 2 shows a sequence alignment of representative members of the two classes, illustrating the absence of TM12 in Tyt1 of *F. nucleatum* (34). This protein was suggested to be a sodium-dependent tyrosine transporter of the oral pathogen *F. nucleatum* subsp. *nucleatum* (The Institute for Genomic Research locus FN1989, chromosome position 492571–493887) based on its linkage to a catabolic enzyme (tyrosine phenol-lyase, β-tyrosinase, 4.1.99.2) open reading frame (The Institute for Genomic Research locus FN1988, chromosome position 491058 – 492440).

After cloning of the *tyt1* gene into a pT7-5 expression plasmid derivative (24), initial transport measurements were inconclusive due to high endogenous aromatic amino acid uptake activity (*i.e.* Phe, Tyr, and Trp) observed in several *E. coli* K12 and B strains tested (data not shown). Expression of *tyt1* from the inducible T5 promoter in a pQE60 derivative revealed only marginal tyrosine accumulation above background (data not shown). To generate a suitable host strain for detailed kinetic and biochemical studies, we used *E. coli* CY15212, a strain already deficient in the three aromatic amino acid uptake systems, Mtr, AroP, and TnaB (25), as the parental strain for the subsequent disruption of the *tyrP* and *pheP* genes. As shown in Fig. 3, disruption of the two additional genes in *E. coli* MQ614 abolished the endogenous tyrosine uptake activity observed in CY15212. Transforming MQ614 with pQ2, a pQE60 derivative containing the *tyt1* gene under control of the T5 promoter, resulted in robust [^{3}H]tyrosine accumulation after induction with isopropyl 1-thio-β-D-galactopyranoside.

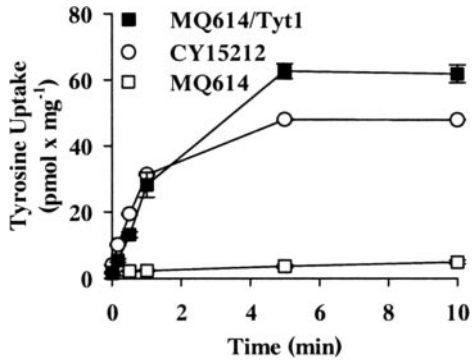

FIGURE 3. **Time course of tyrosine uptake by intact *E. coli*.** Cells were incubated and treated as described under "Experimental Procedures." Uptake of 0.1 μM L-[ring-3,5-^{3}H]tyrosine was assayed in 50 mM Tris/Mes, pH 7.5 in the presence of 100 mM NaCl at 23 °C. 200-μl aliquots of *E. coli* strain CY15212 (○), MQ614 (□), or MQ614/pQ2 (■) at a total cell protein concentration of 0.125 mg/ml were used per rapid filtration assay.

To optimize the experimental conditions for active transport measurements we tested the effect of increasing the pH gradient ($\Delta\tilde{\mu}_{H^+}$) and the membrane potential ($\Delta\Psi$) by decreasing the external pH of the uptake buffer and/or adding 20 mM lactate, methods generally used to stimulate secondary active transport processes (35–37). Surprisingly at pH 6.5 the uptake activity of MQ614 transformed with pQ2 was indistinguishable from MQ614 transformed with the control plasmid (Fig. 4*A*). In contrast, tyrosine transport was dramatically stimulated by increasing the pH with an optimum of pH 8.5 (Fig. 4*B*). Fig. 4*C* shows the effect of varying, simultaneously, the NaCl concentration and the pH. Increasing the NaCl concentration to 100 mM (the concentration used in Fig. 4, *A* and *B*) inhibited Tyt1-catalyzed transport at both pH values tested (Fig. 4*C*). Therefore, with the exception of the analysis of the ion dependence on active tyrosine transport (see Fig. 5), all subsequent uptake experiments were performed at pH 8.5 in the presence of 10 mM NaCl. Under such conditions, with 100 nM [^{3}H]tyrosine, the initial rate of tyrosine transport was ~1500 pmol × mg of cell protein^{-1} × min^{-1}, whereas the steady state of tyrosine accumulation reached about 500 pmol × mg of total cell protein^{-1} after 1 min (see also Fig. 8*A*).

The requirement for Na^+ as the coupling cation is depicted in Fig. 5. Under standard transport conditions (0.1 μM L-[1-^{14}C]tyrosine) the apparent half-maximum stimulation constant of Na^+-driven tyrosine transport ($K_{0.5}^{Na^+}$) was 0.75 ± 0.03 mM with a Hill coefficient of 2 ± 0.2 (Fig. 5*A*, *inset*). At more saturating concentrations of L-[1-^{14}C]tyrosine (1 μM; Fig. 5*A*), the $K_{0.5}^{Na^+}$ was 1.4 ± 0.1 mM (Hill coefficient of 1.9 ± 0.2). Fig. 5*B* shows that the highest transport activity was observed in the presence of Na^+, whereas the chloride anion under these test conditions was dispensable

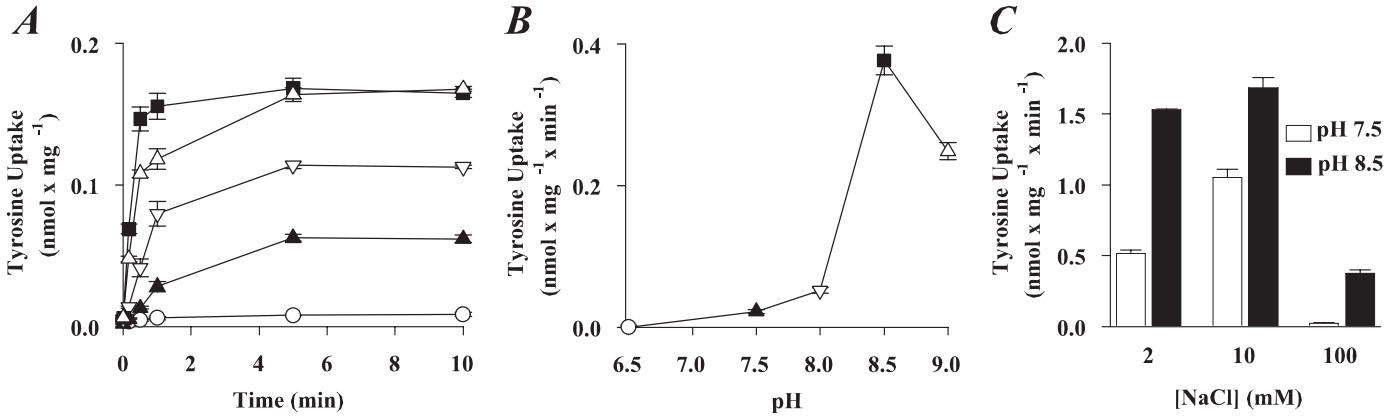

FIGURE 4. **Effect of the pH on Tyt1-mediated tyrosine accumulation.** *A*, time course of L-[1-^{14}C]tyrosine uptake by MQ614/pQ2 was measured in the presence of 100 mM NaCl in 50 mM Tris/Mes, pH 6.5 (○), pH 7.5 (▲), pH 8.0 (▽), pH 8.5 (■), or pH 9.0 (△). *B*, pH dependence of initial rates of L-[1-^{14}C]tyrosine transport by *E. coli* MQ614/pQ2. Initial rates were calculated from the linear portion of tyrosine accumulation between 0 and 10 s shown in *A*. *Symbols* were used accordingly. *C*, initial rates of L-[1-^{14}C]tyrosine uptake were determined in the presence of 2, 10, or 100 mM NaCl in 50 mM Tris/Mes, pH 7.5 (*open bars*) or 8.5 (*closed bars*).

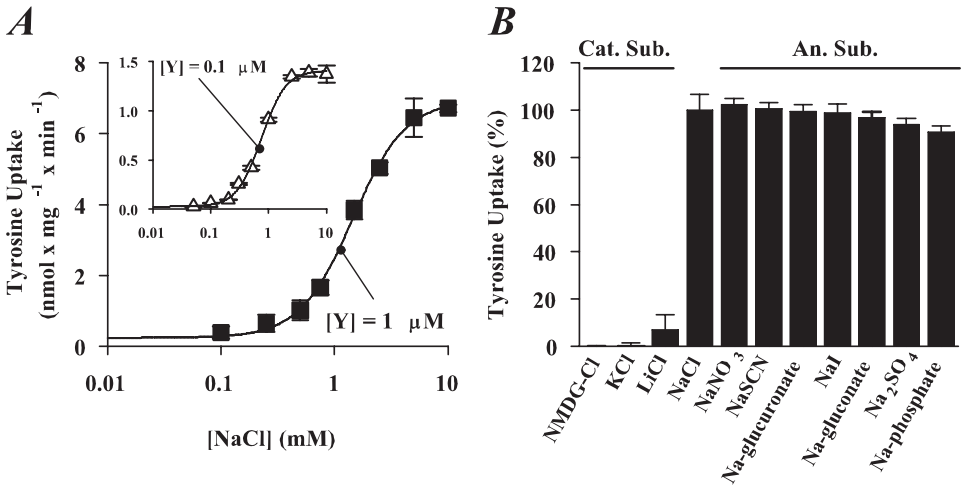

FIGURE 5. **Ion dependence of tyrosine transport by Tyt1.** *A*, stimulation of active tyrosine transport by increasing NaCl concentrations. Initial rates of 1 μM (■) or 0.1 μM (△, *inset*) L-[1-^{14}C]tyrosine transport were measured by varying the NaCl concentration from virtually Na^+-free to 10 mM (equimolar replacement of NaCl with Tris/Mes). The half-maximum activation constant ($K_{0.5}^{Na^+}$) was determined by a least squares fit of the data as 0.75 ± 0.03 mM NaCl (Hill coefficient of 2 ± 0.2) and 1.4 ± 0.1 mM (Hill coefficient of 1.9 ± 0.2) at tyrosine concentrations of 0.1 or 1 μM, respectively. *B*, cation and anion dependence of Tyt1-mediated transport. Initial rates of tyrosine transport (at 0.1 μM final L-[1-^{14}C]tyrosine concentration) were measured in uptake buffer in which 10 mM NaCl was substituted with *N*-methyl-D-glucamine-Cl (*NMDG-Cl*), KCl, or LiCl (cationic substitution (*Cat. Sub.*)) or $NaNO_3$, NaCNS, sodium glucuronate, NaI, sodium gluconate, Na_2SO_4, or sodium phosphate (anionic substitution (*An. Sub.*)).

for function. Similarly chloride was not essential for transport by either LeuT or TnaT (21, 33).

Kinetic characterization of Tyt1-mediated active tyrosine transport in the presence of 10 mM NaCl revealed that tyrosine transport is saturable with a $K_{0.5}^{Tyr}$ of 0.34 ± 0.08 μM and a V_{max}^{Tyr} of 6.9 ± 0.3 nmol × mg of cell protein^{-1} × min^{-1} (Fig. 6*A*; see also Table 1). The specificity of Tyt1-mediated transport was determined by measuring L-[1-^{14}C]tyrosine uptake in the presence of a 100-fold excess, *i.e.* 10 μM, of each of the 20 naturally occurring L-amino acids (Fig. 6*B*) as well as several tyrosine analogues (Fig. 6*C*). With the exception of L-tyrosine, none of the naturally occurring amino acids significantly inhibited Tyt1-catalyzed L-tyrosine uptake. D-Tyrosine, tyramine, 6-hydroxy-DL-(3,4-dihydroxyphenyl)-L-alanine, 5-diiodo-L-tyrosine, and α-methyl-L-tyrosine also failed to inhibit tyrosine uptake. 3-Amino-L-tyrosine and *O*-methyl-L-tyrosine showed weak inhibition (27 and 34% reduction of L-tyrosine transport, respectively, at a concentration of 10 μM), and 3-(3,4-dihyroxyphenyl)-L-alanine reduced transport activity to 40% at 10 μM, consistent with a loss of potency of ~30-fold by the addition of the OH in the 3-position. Note that the absence of the OH in the 4-position (phenylalanine) led to a virtually complete loss of affinity, demonstrating the remarkable specificity of Tyt1 for tyrosine.

At amino acid position 24 in Tyt1 (index position 1.45) is a glycine residue that is highly conserved among the amino acid transporters of the NSS family (See Ref. 38 for a description of the indexing system for NSS.[3] Briefly to facilitate comparison of the NSS sequences, the most conserved position in the sequence alignment is chosen for each TM segment, and this position is assigned the number 50. Other positions are numbered relative to this reference position, *e.g.* positions directly N- and C-terminal are designated as 49 and 51, respectively.)

In the biogenic amine transporters, however, the corresponding residue is an aspartate (see Fig. 2).[3] We showed previously that mutation to Asp of this conserved Gly in TnaT abolished tryptophan transport but did not lead to transport of serotonin (33). Based on the LeuT structure, Yamashita *et al.* (21) proposed that in the biogenic amine transporters the β-carboxyl group of $Asp_{1.45}$ substitutes for the α-carboxyl group of the amino acid substrate and coordinates a Na^+ ion. To test this hypothesis, we replaced Gly-24 in Tyt1 with Asp and assayed transport of tyrosine and the corresponding biogenic amine, tyramine. Whereas the mutation had no significant effect on the amount of Tyt1 in the membrane of MQ614 (based on immunoblot analysis using a monoclonal antibody against the His_{10} tag of each Tyt1 variant (data not shown)), replacement of Gly-$24_{1.45}$ by Asp completely abolished Na^+-driven tyrosine transport (Fig. 7, *left ordinate*) even when tested for 2 h, conditions that have allowed us to observe uptake by dramatically impaired TnaT mutants for which no transport could be measured at 2 min (data not shown). However, as for TnaT, this mutation did not change the amino acid transporter into one that catalyzes amine (tyramine) transport (Fig. 7, *right ordinate*). Lowering the pH of the uptake buffer or replacing the coupling cation Na^+ with Li^+ also did not produce tyramine transport by the $G24_{1.45}D$ mutant (data not shown).

Tyt1 contains two endogenous cysteines at positions 18 and 238 (index positions 1.39 and 6.65, respectively; see also Fig. 2) near the intracellular ends of TM1 and TM6, respectively. In a homology model of Tyt1 based on the LeuT structure, these cysteines face each other deep within the core of the cytoplasmic part of the transporter (see Fig. 9*A*). Nonetheless in preliminary experiments we observed that in intact *E. coli*, sodium-dependent tyrosine transport by the wild type Tyt1 was rapidly eliminated by the membrane-permeant sulfhydryl-alkylating reagent NEM (see below). Replacing Cys-$18_{1.39}$ with Ala and/or Cys-$238_{6.65}$ with Phe did not significantly alter the initial rate and steady state of tyrosine transport (Fig. 8*A*). Kinetic analyses of Na^+-coupled tyrosine transport by Tyt1-C18A, -C238F, and -CL revealed that $K_{0.5}^{Tyr}$ and V_{max}^{Tyr} were not significantly altered when compared with Tyt1 wild type (Table 1).

Whereas Tyt1-CL activity was unaffected by NEM, Tyt1-WT, Tyt1-C18A, and Tyt1-C238F showed a strong sensitivity toward this sulfhydryl reagent when the reaction was performed in Na^+-free Tris/MES buffer (Fig. 8*B*). A similar result was obtained when the NEM reaction was performed in the presence of 10 μM tyrosine (also in the absence of NaCl). Remarkably, however, when NEM was added in the presence of 10 mM NaCl, its inhibitory effect on tyrosine

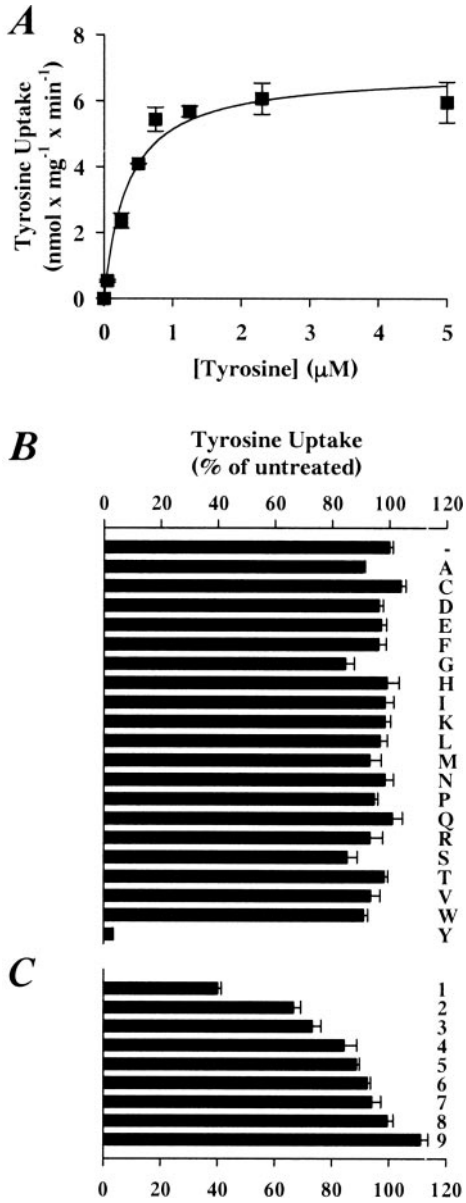

FIGURE 6. **Kinetic analysis of tyrosine uptake by Tyt1.** *A*, initial rates of tyrosine transport were measured at L-[1-^{14}C]tyrosine concentrations between 0.05 and 5 μM in the presence of 50 mM Tris/Mes, pH 8.5 plus 10 mM NaCl. A non-linear least squares fit of the data yielded a $K_{0.5}^{Tyr}$ of 0.34 ± 0.08 μM and a V_{max}^{Tyr} of 6.9 ± 0.3 nmol × mg of protein^{-1} × min^{-1}. *B* and *C*, substrate specificity of Tyt1. Uptake of 0.1 μM L-[1-^{14}C]tyrosine by intact cells of *E. coli* MQ614 expressing Tyt1 was assayed in the presence or absence of a 10 μM concentration of the indicated compound for 1 min. Data are presented as the percentage of the untreated control (−). *B*, effect of L-amino acids on Tyt1-mediated tyrosine transport. *Letters* represent the standard single letter amino acid code. *C*, effect of tyrosine analogues on L-tyrosine transport by Tyt1. *Numbers* indicate the following compounds: 3-(3,4-dihydroxyphenyl)-L-alanine (*1*); *O*-methyl-L-tyrosine (*2*); 3-amino-L-tyrosine (*3*); D-tyrosine (*4*); α-methyl-L-tyrosine (*5*); 5-diiodo-L-tyrosine (*6*); 6-hydroxy-DL-(3,4-dihydroxyphenyl)-L-alanine (*7*); tyramine (*8*); and dopamine (*9*).

TABLE 1

Tyrosine kinetics of Tyt1 variants

Initial rates of L-[1-^{14}C]tyrosine uptake by *E. coli* MQ614 harboring the given Tyt1 variant were measured at tyrosine concentrations from 0.05 to 10 μM in the presence of 10 mM NaCl. Kinetic constants were determined by a least squares fit of the data from a typical experiment (data points in triplicate), and errors represent S.E. of the fit.

Tyt1	WT	CL	C238F	C18A
$K_{0.5}^{Tyr}$ (μM)	0.34 ± 0.08	0.21 ± 0.04	0.29 ± 0.04	0.27 ± 0.05
V_{max}^{Tyr} (nmol × mg^{-1} × min^{-1})	6.9 ± 0.3	5.9 ± 0.3	6.2 ± 0.3	6.6 ± 0.3

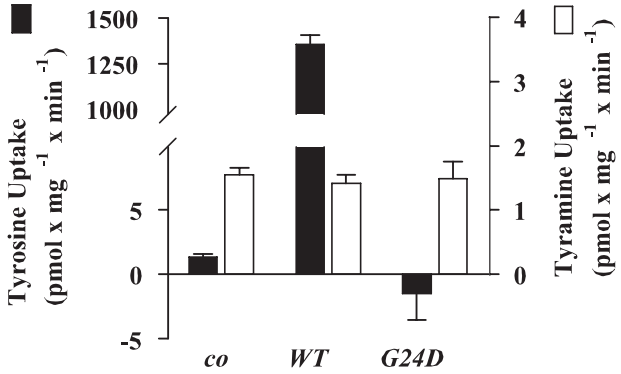

FIGURE 7. **Effect of the G24D mutation in Tyt1.** *E. coli* MQ614 harboring Tyt1-WT, Tyt1-G24D, or a control plasmid (*co*) were prepared for transport measurements as described under "Experimental Procedures." Initial rates of 0.1 μM L-[1-^{14}C]tyrosine transport (*filled bars*, *left ordinate*) or 0.1 μM [^{3}H]tyramine (*open bars*, *right ordinate*) were determined in 50 mM Tris/Mes, pH 8.5 plus 10 mM NaCl.

transport by Tyt1-WT, Tyt1-C18A, and Tyt1-C238F was greatly diminished (Fig. 8*B*). This diminished inhibition resulted from a decrease in the reactivity of the cysteines with NEM because high concentrations of NEM could still inhibit transport even in the presence of NaCl (data not shown). When NEM was added in the presence of both NaCl and tyrosine, thereby enabling transport, the inhibitory effect of NEM was increased, consistent with an increase in the accessibility of each of the endogenous cysteines during the transport cycle.

DISCUSSION

Here we present data on the function of a new member of the NSS family, Tyt1 of *F. nucleatum*. Based on the sequence homology to the NSS family and the localization of the *tyt1* gene adjacent to a catabolic gene locus (β-tyrosinase gene) on the *F. nucleatum* chromosome, Tyt1 was suggested to function as a tyrosine transporter (34). We cloned the *tyt1* gene and overexpressed the protein in a novel *E. coli* strain, MQ614, which we engineered to be devoid of all aromatic amino acid transport. Our analysis revealed that Tyt1 is a functional Na^+-dependent tyrosine transporter. Tyt1 is representative of ~70% of prokaryotic NSS members that are predicted to consist of 11 TMs in contrast to the remaining prokaryotic NSSs and eukaryotic NSSs that contain a 12th transmembrane segment. The function of Tyt1, despite the absence of TM12, suggests that this large 11-TM subfamily of NSS contains functional transporters and not pseudogenes. Interestingly the protein core of LeuT consists of the first 10 of 12 transmembrane segments with segments 1–5 related to segments 6–10 by a pseudo-2-fold axis in the membrane plane (21). TM11 and TM12 are located on the periphery of the LeuT structure and are not known to play a critical role in binding or transport (21). Thus, our sequence analysis and experimental data are consistent with an evolutionary divergence in the structure of the C-terminal part of the protein while conserving the functional core.

Although Tyt1 lacks TM12, its overall sequence homology,

the conservation of key residues (Ref. 38),[3] and its functional properties clearly identify it as a member of the NSS family. Like most NSS family members, Tyt1-mediated tyrosine transport is highly selective and exhibits a substrate affinity in the 10^{-7}–10^{-6} M range. In addition, the ion dependence of Tyt1 resembles that of DAT, SERT, and NET in so far as these transporters exhibit a strict dependence on Na^+ as the coupling ion for substrate uptake (3, 22). Whereas several other Na^+-dependent transporters can substitute Li^+ or even H^+ as the coupling ion (MelB (39), sodium/proline transporter of *E. coli* (40), human SGLT (27), and rabbit SGLT (41)), H^+ and K^+ failed to drive substrate uptake by Tyt1, whereas Li^+ showed small but significant transport activation.

In contrast to DAT, NET, and SERT (3, 22, 42), however, Tyt1 activity is unaffected by the presence or absence of Cl^-. A similar lack of chloride ion dependence was observed for TnaT (33) and LeuT (21). Although a chloride ion was detected in the crystal structure of LeuT (bound to the outer surface of the protein), a role for this ion in (co)transport remains enigmatic.

The high apparent affinity of Tyt1 for Na^+ in the ~1 mM range may reflect the physiological role of Tyt1 in the oral pathogen *F. nucleatum* as a transport system for the essential amino acid tyrosine (34) because salivary sodium concentrations are 10–20-fold lower than typical extracellular sodium concentrations (43). Several other bacterial transport systems with an apparent Na^+ affinity in the micromolar range also have been detected (29, 44, 45). However, the strong inhibitory effect of NaCl concentrations above 10 mM on Tyt1 activity has not been observed in other bacterial symporters with a high Na^+ affinity (29, 40).

Tyt1 activity peaked at a pH of 8.5. A similar tendency has been observed for other members of the NSS family, namely mouse B^0AT2 (46), KAAT1 (47), and CAATCH-1 (48), the latter two of which are situated in a nutrient absorptive epithelium of *Manduca sexta* and are exposed to high transmembrane voltages and alkaline pH. The Tyt1 pH dependence might also result, in full or part, from the effect of pH on NhaA, the major Na^+/H^+ antiporter in *E. coli* (the expression system used for the present study). The physiological role of this transporter is the extrusion of intracellular Na^+ from cells coupled to import of H^+. NhaA function is stimulated ~2000-fold by increasing the external pH from 6.5 to 8.5, a pattern similar to that of Tyt1 activity (compare Fig. 6 in Ref. 49 and Fig. 4*B* in the present study). Therefore, increased NhaA activity at higher pH might lead to increased Na^+ extrusion and a lower intracellular Na^+ concentration and in turn to a larger Na^+ driving force and increased tyrosine uptake. Differentiating these mechanisms will require study of purified Tyt1 reconstituted into proteoliposomes.

Our results support a Na^+/tyrosine cotransport (symport) mechanism by Tyt1 with the electrochemical Na^+ gradient as the immediate driving force for substrate uptake. The Hill coefficient of ~2 is consistent with an apparent stoichiometry of 2 Na^+:1 tyrosine for coupled uptake. This is in line with much functional data in other NSSs, such as the Hill coefficient of 2 for sodium in dopamine transport by DAT (3, 50) as well as the identification of two bound Na^+ ions in the crystal structure of LeuT (21). In this

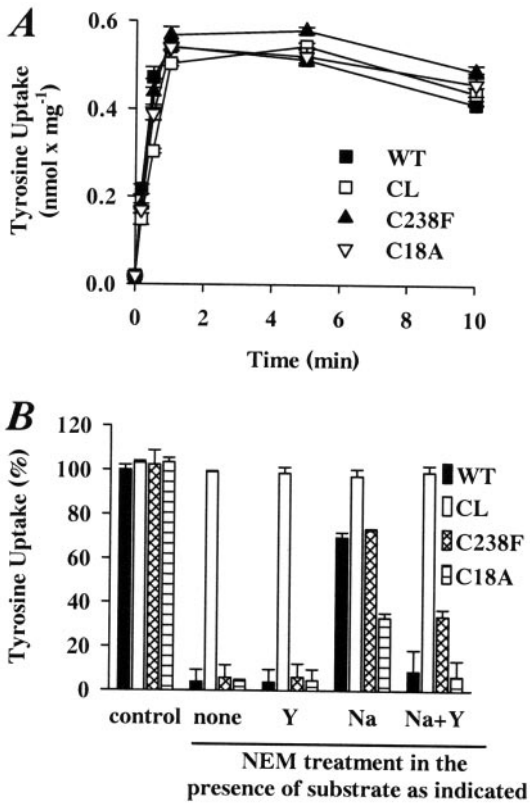

FIGURE 8. **Role of cysteine residues in Tyt1.** *A*, time course of tyrosine uptake by intact *E. coli* MQ614 harboring Tyt1-WT (■), Tyt1-CL (□), Tyt1-C238F (▲), or Tyt1-C18A (▽). Uptake of 0.1 μM L-[1-^{14}H]tyrosine was assayed in 50 mM Tris/Mes, pH 8.5 in the presence of 10 mM NaCl at 23 °C. *B*, effect of NEM on Tyt1 activity. Cells of *E. coli* MQ614 producing Tyt1-WT, -CL, -C18A, or -C238F were cultivated and treated for transport as described under "Experimental Procedures." Prior to uptake measurements, cells were incubated with NEM in the absence (*none*) or presence of 10 μM L-tyrosine (*Y*), 10 mM NaCl (*Na*), or 10 mM NaCl, 10 μM L-tyrosine (*Na+Y*) for 5 min at 23 °C. The concentration of NEM was adjusted for each NEM-sensitive Tyt1 variant (Tyt1-WT and -C18A: 1 mM; -C238F: 1.5 mM) to produce ~95% reduction of active tyrosine transport in the absence of substrate compared with non-treated cells. As control, cells expressing Tyt1-CL were treated with 1.5 mM NEM. Means of data, except data of untreated cells (control) and cells expressing Tyt1-CL, were significantly different with $p < 0.05$ as determined by one-way analysis of variance with posthoc analysis by Tukey's test.

structure, the carboxyl oxygen of the substrate, leucine, forms an ion pair with one Na^+ (Na1). The authors proposed that the β-carboxyl group of $Asp_{1.45}$, which is conserved among the eukaryotic biogenic amine transporters, could substitute for the carboxyl group of leucine and thereby coordinate Na1 (21). Replacing the corresponding residue in Tyt1 (Gly-$24_{1.45}$) with Asp impaired tyrosine transport, consistent with our previous results for mutation of the aligned position in TnaT (33). However, despite the presence of the Tyt1-G24D protein in the membrane, this mutant did not transport tyramine, indicating that the mechanism of biogenic amine transport requires more than substitution of the residue at position 1.45. Moreover using a newly developed method for measuring substrate binding,[4] we have determined that neither tyramine nor tyrosine bind to Tyt1-G24D and that Tyt1-WT binds tyrosine but not tyramine. Thus, it seems likely that an Asp must be present at position 1.45 for biogenic amine

[4] M. Quick and J. A. Javitch, in preparation.

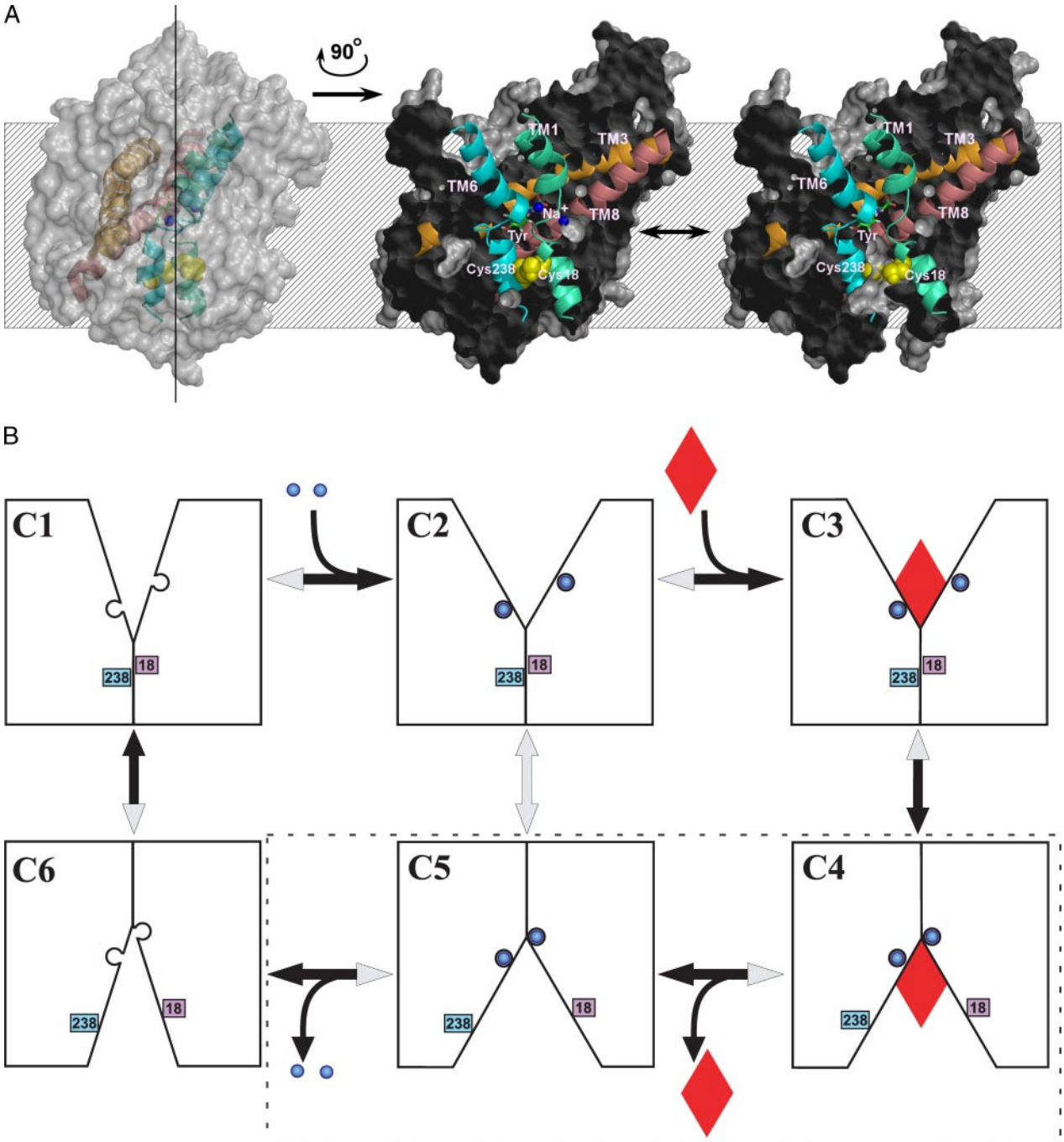

FIGURE 9. **State-dependent accessibility of Cys-18 and Cys-238.** *A*, a molecular model of Tyt1 with tyrosine, shown in the *left* and *middle panels*, was constructed with the homology modeling algorithm Modeler 8v1 (64) based on the crystal structure of LeuT (21) and the proposed sequence alignment (T. Beuming, L. Shi, J. A. Javitch, and H. Weinstein, in preparation). The figure was prepared with InsightII (Accelrys, San Diego, CA) and PyMOL (DeLano Scientific LLC). The molecular models in all three panels are rendered with molecular surfaces obtained with a probe radius of 1.4 Å. The transmembrane segments, TM1, TM3, TM6, and TM8, which contact the substrate tyrosine, are shown as *ribbons*. Tyrosine is rendered in *stick* representation, and Cys-18 and Cys-238 are in *space-filling* representations. In the *left panel*, the molecular surface is made partially transparent to depict the positioning and orientations of the TMs, tyrosine, two sodium ions (*blue balls*), and the two endogenous cysteines (*yellow* Corey-Pauling-Koltun) buried within the core of the Tyt1 model. In the *middle panel*, the model is rotated clockwise by 90° around an axis in the plane of the page, and the molecular surface is clipped to a plane whose position is indicated by the *vertical line* in the *left panel*. In the *right panel*, the model is shown in the same orientation and clipping as in the *middle panel*. To illustrate the increased accessibility of Cys-18 and Cys-238 from the intracellular milieu in the absence of Na^+ as well as during transport, TM1 was manually repositioned to reflect a movement away from TM6. Such a rearrangement would open a potential crevice in which Cys-18 and Cys-238 become accessible to the aqueous milieu. This crevice does not exist in the corresponding region of the crystal structure of LeuT but illustrates the type of opening expected for a transport pathway that must be associated with the inward facing conformation of the transporter. *B*, kinetic scheme for Na^+/tyrosine cotransport. The six-state binding model consists of the empty transporter (states C1 and C6), the Na^+-bound states (C2 and C5), and the Na^+- and tyrosine-bound states (C3 and C4) facing the external (C1–C3) or the internal (C4–C6) surface of the membrane. Binding of two Na^+ ions (*blue balls*) to Tyt1 (C1 → C2) organizes the tyrosine binding site. Binding of tyrosine (*red diamond*) causes a conformational change leading to C3 and subsequently to C4. The sequence of the physiological transport cycle is represented in clockwise fashion (*black arrows*), whereas the reverse reactions are indicated by *gray arrowheads*. Note that there is no experimental evidence for the unbinding sequence of tyrosine and Na^+ ions (states C4 and C5, *dashed rectangle*) as well as for the C2 ↔ C5 transition (Na^+ leak; *gray arrow*). The position of cysteine residues 18 and 238 (index positions 1.39 and 6.65, respectively) are highlighted.

binding and transport, but other changes in the protein are necessary for amine recognition and transport.

Structural information at the atomic level is important to elucidate the architecture of transport proteins and the location of bound substrates, but without functional data the structure of a single conformational state provides few clues about the dynamics of a transport protein during the transport cycle. Tyt1 contains two endogenous cysteine residues located at position $18_{1.39}$ and $238_{6.65}$. These positions align with amino acid residues Met-$18_{1.39}$ and Tyr-$265_{6.65}$ in LeuT that are located within the cytoplasmic segments of TM1a and TM6b, respectively (21). In Tyt1, replacement of either or both of these Cys residues yielded a functional protein with transport kinetics comparable to Tyt1 wild type (Fig. 8*A*).

Probing the structural arrangements associated with sodium binding, we found that in the presence of 10 mM NaCl, WT and the single cysteine mutants were protected against NEM inactivation (Fig. 8*B*). This is consistent with a decreased accessibility of these endogenous cysteines in the sodium-bound state. We have observed a parallel increase in the accessibility to externally applied impermeant sulfhydryl reagents of substituted Cys in TM3 near the binding site in TnaT.[5] Thus, sodium appears to produce a "closed-inward/open-outward" configuration of the transporter, poised to bind the substrate from the extracellular milieu.

In contrast, in the absence of sodium, tyrosine had no effect on reaction of Tyt1 with NEM (Fig. 8*B*), consistent with an ordered binding scheme in which the binding of sodium organizes the transporter structure to allow tyrosine binding. This result also parallels predictions for other secondary transport proteins for which an alternate-access ordered binding model has been demonstrated (SGLT1 (27, 51, 52), Na^+/iodide symporter (53), MelB (54), and NaPi-2 (55)). It is also consistent with the inference that initial binding of Na^+ ions to LeuT is required to organize the substrate binding site, particularly the partially unwound regions in TM1 and TM6 that make an essential contribution to binding (21). Our binding studies indicate that sodium is also essential for tyrosine binding.[4] Curiously there is evidence suggesting that dopamine and serotonin can interact with DAT and SERT in the absence of sodium (22, 56), suggesting that there may be subtle differences in dynamics within the NSS family, but other reports are consistent with an ordered binding scheme for DAT as well (57).

Addition of Na^+ together with tyrosine facilitates reaction of WT and the single-Cys Tyt1 mutants with NEM. This is consistent with increased accessibility of cytoplasmic NEM to the transport pathway that is opened during the transport cycle. A molecular model of Tyt1 based on the homology to LeuT (see Fig. 9*A* for details) shows the endogenous Cys residues at positions $18_{1.39}$ and $238_{6.65}$ buried deep within the structure when the cytoplasmic gate is closed (Fig. 9*A*, *left* and *middle panels*); these cysteines would not be expected to have significant reactivity in this configuration. But our data from accessibility studies are consistent with the type of kinetic model proposed for SGLT1 (51) (Fig. 9*B*) in which, in the absence of sodium, the structure fluctuates between an outward facing and an inward facing configuration (C1 and C6, respectively). According to the model, this would make Cys-$18_{1.39}$ and Cys-$238_{6.65}$ intermittently accessible to react with intracellular NEM. Sodium facilitates the transition to C2 (sodium-bound state), thereby shifting the transporter population away from C6 into an outward facing conformation. As a consequence, the accessibility of Cys-$18_{1.39}$ and Cys-$238_{6.65}$ to NEM is decreased by burying them within the protein interior, likely in a configuration similar to that seen in the LeuT structure (compare Fig. 9*A*; note that the LeuT structure presumably represents a closed outward and closed inward state trapped between C3 and C4). When tyrosine is added in the presence of sodium (state C3), transport ensues, making Cys-$18_{1.39}$ and Cys-$238_{6.65}$ accessible from the cytoplasm (states C4, C5, and/or C6).

Taken together, these results identify the cytoplasmic ends of TM1 and TM6 as dynamic contributors to the transport pathway. Interestingly in DAT the nearby residue Cys-$342_{7.27}$ (10 residues after 6.65) was inaccessible to a membrane-permeant sulfhydryl reagent applied in the presence of extracellular sodium but became accessible during the transport cycle when the substrate tyramine was added (58). This cysteine was also protected from reaction when cocaine was present, consistent with a model in which cocaine stabilizes an outward facing conformation of DAT (58). This dynamic rearrangement is underscored by our findings that cocaine is not a neutral blocker but rather alters the conformation of extracellular and intracellular cysteines in DAT (59, 60). That cocaine binding is greatly enhanced by sodium (61) is also consistent with cocaine binding preferentially to a C2- or C3-like configuration.

The detailed conformational changes that are associated with opening of the transport pathway must be determined experimentally. Yamashita *et al.* (21) have proposed that movement of TM1 and/or TM6 around their unwound regions might be part of the gating mechanism (21). Our results lead us to speculate that the opening of the translocation pathway involves the separation of the intracellular ends of TM1 and TM6, which makes Cys-$18_{1.39}$ and Cys-$238_{6.65}$ accessible from the internal aqueous milieu. Fig. 9*A*, *right panel*, illustrates such an "inward facing" conformation.

Acknowledgments—We thank Mark Sonders for critical reading of the manuscript and Lucy Skrabanek for helpful discussion of the phylogenetic analysis.

REFERENCES

1. Rudnick, G., and Clark, J. (1993) *Biochim. Biophys. Acta* **1144,** 249–263
2. Rudnick, G. (ed) (2002) in *Neurotransmitter Transporters: Structure, Function and Regulation* (Reith, M. E. A., ed) 2nd Ed., Humana Press Inc., Totowa, NJ
3. Gu, H., Wall, S. C., and Rudnick, G. (1994) *J. Biol. Chem.* **269,** 7124–7130
4. Norregaard, L., and Gether, U. (2001) *Curr. Opin. Drug. Discov. Dev.* **4,** 591–601
5. Torres, G. E., Gainetdinov, R. R., and Caron, M. G. (2003) *Nat. Rev. Neurosci.* **4,** 13–25
6. Saier, M. H., Jr. (1999) *J. Cell Biochem.* **75,** Suppl. 32/33, 84–94
7. Masson, J., Sagne, C., Hamon, M., and El Mestikawy, S. (1999) *Pharmacol. Rev.* **51,** 439–464
8. Sonders, M. S., Quick, M., and Javitch, J. A. (2005) *Curr. Opin. Neurobiol.* **15,** 296–304

[5] N. R. Goldberg and J. A. Javitch, in preparation.

9. Chen, N. H., Reith, M. E., and Quick, M. W. (2004) *Pfluegers Arch. Eur. J. Physiol.* **447,** 519–531
10. Amara, S. G., and Sonders, M. S. (1998) *Drug Alcohol Depend.* **51,** 87–96
11. Iversen, L. (2006) *Br. J. Pharmacol.* **147,** S82–S88
12. Guastella, J., Nelson, N., Nelson, H., Czyzyk, L., Keynan, S., Miedel, M. C., Davidson, N., Lester, H. A., and Kanner, B. I. (1990) *Science* **249,** 1303–1306
13. Kilty, J. E., Lorang, D., and Amara, S. G. (1991) *Science* **254,** 578–579
14. Blakely, R. D., Berson, H. E., Fremeau, R. T., Jr., Caron, M. G., Peek, M. M., Prince, H. K., and Bradley, C. C. (1991) *Nature* **354,** 66–70
15. Pacholczyk, T., Blakely, R. D., and Amara, S. G. (1991) *Nature* **350,** 350–354
16. Tate, C. G. (2001) *FEBS Lett.* **504,** 94–98
17. Tate, C. G., Haase, J., Baker, C., Boorsma, M., Magnani, F., Vallis, Y., and Williams, D. C. (2003) *Biochim. Biophys. Acta* **1610,** 141–153
18. Rees, D. C., Chang, G., and Spencer, R. H. (2000) *J. Biol. Chem.* **275,** 713–716
19. Doyle, D. A., Morais Cabral, J., Pfuetzner, R. A., Kuo, A., Gulbis, J. M., Cohen, S. L., Chait, B. T., and MacKinnon, R. (1998) *Science* **280,** 69–77
20. Chang, G., Spencer, R. H., Lee, A. T., Barclay, M. T., and Rees, D. C. (1998) *Science* **282,** 2220–2226
21. Yamashita, A., Singh, S. K., Kawate, T., Jin, Y., and Gouaux, E. (2005) *Nature* **437,** 215–223
22. Sonders, M. S., Zhu, S. J., Zahniser, N. R., Kavanaugh, M. P., and Amara, S. G. (1997) *J. Neurosci.* **17,** 960–974
23. Mager, S., Naeve, J., Quick, M., Labarca, C., Davidson, N., and Lester, H. A. (1993) *Neuron* **10,** 177–188
24. Quick, M., and Wright, E. M. (2002) *Proc. Natl. Acad. Sci. U. S. A.* **99,** 8597–8601
25. Yanofsky, C., Horn, V., and Gollnick, P. (1991) *J. Bacteriol.* **173,** 6009–6017
26. Datsenko, K. A., and Wanner, B. L. (2000) *Proc. Natl. Acad. Sci. U. S. A.* **97,** 6640–6645
27. Quick, M., Loo, D. D., and Wright, E. M. (2001) *J. Biol. Chem.* **276,** 1728–1734
28. Miller, J. H. (1992) *A Short Course in Bacterial Genetics. A Laboratory Manual and Handbook for Escherichia coli and Related Bacteria*, Cold Spring Harbor Laboratory, Cold Spring Harbor, NY
29. Quick, M., and Jung, H. (1997) *Biochemistry* **36,** 4631–4636
30. Quick, M., Tebbe, S., and Jung, H. (1996) *Eur. J. Biochem.* **239,** 732–736
31. Tusnády, G. E., and Simon, I. (2001) *Bioinformatics* **17,** 849–850
32. Sonnhammer, E. L., von Heijne, G., and Krogh, A. (1998) *Proc. Int. Conf. Intell. Syst. Mol. Biol.* **6,** 175–182
33. Androutsellis-Theotokis, A., Goldberg, N. R., Ueda, K., Beppu, T., Beckman, M. L., Das, S., Javitch, J. A., and Rudnick, G. (2003) *J. Biol. Chem.* **278,** 12703–12709
34. Kapatral, V., Anderson, I., Ivanova, N., Reznik, G., Los, T., Lykidis, A., Bhattacharyya, A., Bartman, A., Gardner, W., Grechkin, G., Zhu, L., Vasieva, O., Chu, L., Kogan, Y., Chaga, O., Goltsman, E., Bernal, A., Larsen, N., D'Souza, M., Walunas, T., Pusch, G., Haselkorn, R., Fonstein, M., Kyrpides, N., and Overbeek, R. (2002) *J. Bacteriol.* **184,** 2005–2018
35. Konings, W. N., Barnes, E. M., Jr., and Kaback, H. R. (1971) *J. Biol. Chem.* **246,** 5857–5861
36. Kaback, H. R., and Barnes, E. M., Jr. (1971) *J. Biol. Chem.* **246,** 5523–5531
37. Barnes, E. M., Jr., and Kaback, H. R. (1970) *Proc. Natl. Acad. Sci. U. S. A.* **66,** 1190–1198
38. Goldberg, N. R., Beuming, T., Soyer, O. S., Goldstein, R. A., Weinstein, H., and Javitch, J. A. (2003) *Eur. J. Pharmacol.* **479,** 3–12
39. Bassilana, M., Pourcher, T., and Leblanc, G. (1987) *J. Biol. Chem.* **262,** 16865–16870
40. Quick, M., and Jung, H. (1998) *Biochemistry* **37,** 13800–13806
41. Hirayama, B. A., Loo, D. D., and Wright, E. M. (1994) *J. Biol. Chem.* **269,** 21407–21410
42. Corey, J. L., Quick, M. W., Davidson, N., Lester, H. A., and Guastella, J. (1994) *Proc. Natl. Acad. Sci. U. S. A.* **91,** 1188–1192
43. Jensdottir, T., Nauntofte, B., Buchwald, C., and Bardow, A. (2005) *Caries Res.* **39,** 468–474
44. Damiano-Forano, E., Bassilana, M., and Leblanc, G. (1986) *J. Biol. Chem.* **261,** 6893–6899
45. van der Rest, M. E., Molenaar, D., and Konings, W. N. (1992) *J. Bacteriol.* **174,** 4893–4898
46. Bröer, A., Tietze, N., Kowalczuk, S., Chubb, S., Munzinger, M., Bak, L. K., and Bröer, S. (2006) *Biochem. J.* **393,** 421–430
47. Castagna, M., Shayakul, C., Trotti, D., Sacchi, V. F., Harvey, W. R., and Hediger, M. A. (1998) *Proc. Natl. Acad. Sci. U. S. A.* **95,** 5395–5400
48. Feldman, D. H., Harvey, W. R., and Stevens, B. R. (2000) *J. Biol. Chem.* **275,** 24518–24526
49. Taglicht, D., Padan, E., and Schuldiner, S. (1991) *J. Biol. Chem.* **266,** 11289–11294
50. Krueger, B. K. (1990) *J. Neurochem.* **55,** 260–267
51. Parent, L., Supplisson, S., Loo, D. D., and Wright, E. M. (1992) *J. Membr. Biol.* **125,** 63–79
52. Loo, D. D., Hirayama, B. A., Cha, A., Bezanilla, F., and Wright, E. M. (2005) *J. Gen. Physiol.* **125,** 13–36
53. Eskandari, S., Loo, D. D., Dai, G., Levy, O., Wright, E. M., and Carrasco, N. (1997) *J. Biol. Chem.* **272,** 27230–27238
54. Meyer-Lipp, K., Ganea, C., Pourcher, T., Leblanc, G., and Fendler, K. (2004) *Biochemistry* **43,** 12606–12613
55. Forster, I., Hernando, N., Biber, J., and Murer, H. (1998) *J. Gen. Physiol.* **112,** 1–18
56. Mager, S., Min, C., Henry, D. J., Chavkin, C., Hoffman, B. J., Davidson, N., and Lester, H. A. (1994) *Neuron* **12,** 845–859
57. Schenk, J. O., Wright, C., and Bjorklund, N. (2005) *J. Neurosci. Methods* **143,** 41–47
58. Chen, N., Ferrer, J. V., Javitch, J. A., and Justice, J. B., Jr. (2000) *J. Biol. Chem.* **275,** 1608–1614
59. Ferrer, J. V., and Javitch, J. A. (1998) *Proc. Natl. Acad. Sci. U. S. A.* **95,** 9238–9243
60. Reith, M. E., Berfield, J. L., Wang, L. C., Ferrer, J. V., and Javitch, J. A. (2001) *J. Biol. Chem.* **276,** 29012–29018
61. Li, L. B., Cui, X. N., and Reith, M. A. (2002) *Naunyn-Schmiedeberg's Arch. Pharmacol.* **365,** 303–311
62. Felsenstein, J. (2005) *PHYLIP (Phylogeny Inference Package)*, Version 3.6, Department of Genome Sciences, University of Washington, Seattle, WA
63. Do, C. B., Mahabhashyam, M. S. P., Brudno, M., and Batzoglou, S. (2005) *Genome Res.* **15,** 330–340
64. Sali, A., and Blundell, T. L. (1993) *J. Mol. Biol.* **234,** 779–815